$\Omega_b^- \to (\Xi_c^+ K^-)\pi^-$ decay and the Ω_c states

V. R. Debastiani,[1,*] J. M. Dias,[1,2,†] Wei-Hong Liang,[3,‡] and E. Oset[1,§]

[1]*Departamento de Física Teórica and IFIC, Centro Mixto Universidad de Valencia—CSIC, Institutos de Investigación de Paterna, Apartado 22085, 46071 Valencia, Spain*

[2]*Instituto de Física, Universidade de São Paulo, Rua do Matão, 1371, Butantã, CEP 05508-090, São Paulo, São Paulo, Brazil*

[3]*Department of Physics, Guangxi Normal University, Guilin 541004, China*

(Received 25 June 2018; published 26 November 2018)

We study the weak decay $\Omega_b^- \to (\Xi_c^+ K^-)\pi^-$, in view of the narrow Ω_c states recently measured by the LHCb Collaboration and later confirmed by the Belle Collaboration. The $\Omega_c(3050)$ and $\Omega_c(3090)$ are described as meson-baryon molecular states, using an extension of the local hidden gauge approach in coupled channels. We investigate the ΞD, $\Xi_c \bar{K}$, and $\Xi_c' \bar{K}$ invariant mass distributions making predictions that could be confronted with future experiments, providing useful information that could help determine the quantum numbers and nature of these states.

DOI: 10.1103/PhysRevD.98.094022

I. INTRODUCTION

The recent discovery of five narrow Ω_c states by the LHCb Collaboration [1] in pp collisions, also recently confirmed by the Belle Collaboration [2] in e^+e^- collisions, motivated an increasing amount of theoretical work with different proposals for their structure. In particular, the correct assignment of quantum numbers J^P remains an open question, and it could be the key to understand the nature of these states.

Predictions using quark models for such states and related ones were done in Refs. [3–20], with most proposing a diquark-quark structure $(ss)c$. Other methods have also been employed to study these states, as QCD sum rules in Refs. [21–27] and lattice QCD in Ref. [28]. Pentaquark options have been suggested in Refs. [29–34]. Some works have emphasized the value of decay properties to obtain information on the nature of these states [35–37], and a discussion on the possible quantum numbers was given in Ref. [38].

On the other hand, some of these states could actually be pentaquarklike molecules, dynamically generated from meson-baryon interactions in coupled channels with charm $C = 1$, strangeness $S = -2$, and isospin $I = 0$. Predictions in the molecular picture using coupled channels of meson-baryon interactions were done in Refs. [39–41]. In this picture the interaction in the S wave of baryons with spin-parity $J^P = 1/2^+$ or $J^P = 3/2^+$ with pseudoscalar mesons leads to meson-baryon systems with $J^P = 1/2^-$ and $J^P = 3/2^-$, respectively. Channels with vector mesons instead of pseudoscalars can also be included resulting in $J^P = 1/2^-, 3/2^-$, and $5/2^-$. However, most of the recent works adopting this picture manage to relate two or three of the new Ω_c states to meson-baryon systems with $J^P = 1/2^-$ and $J^P = 3/2^-$, dominated by the pseudoscalar-baryon channels.

In Ref. [41] an $SU(6)_{lsf} \times$ HQSS model (HQSS stands for heavy quark spin symmetry) extending the Weinberg-Tomozawa πN interaction was employed to make a systematic study of many possible meson-baryon systems. In Ref. [42] the renormalization scheme of Ref. [41] was reviewed, performing an update of the results of the $C = 1$, $S = -2$, and $I = 0$ sector in view of the new experimental data. The updated results indicate that one can relate the $\Omega_c(3000)$ to a state with $J^P = 1/2^-$ and the $\Omega_c(3050)$ to another state with $J^P = 3/2^-$, with hints that the $\Omega_c(3090)$ or $\Omega_c(3119)$ could also have $J^P = 1/2^-$.

In Ref. [40] the molecular picture was developed using $SU(4)$ symmetry to extend the interaction described by vector meson exchange in the local hidden gauge approach. This work was also reviewed under the light of the new experimental data and an updated study was made in Ref. [43], where it was shown that the $\Omega_c(3050)$ and $\Omega_c(3090)$ can both be related to meson-baryon resonances with $J^P = 1/2^-$, stemming from pseudoscalar-baryon $(1/2^+)$ interaction.

A similar approach that also describes the meson-baryon interaction through vector meson exchange was recently

*vinicius.rodrigues@ific.uv.es
†jdias@if.usp.br
‡liangwh@gxnu.edu.cn
§eulogio.oset@ific.uv.es

developed in Ref. [44], using an extension of the local hidden gauge approach [45–49] and taking into account the spin-flavor wave functions of the baryons. In the present work we will follow the description of the Ω_c states of Ref. [44]; extensive discussions on the methods and results can be found there, as well as predictions of higher energy states of meson-baryon nature. We shall discuss this framework in the next section. A remarkable agreement of both masses and widths of the $\Omega_c(3050)$ and $\Omega_c(3090)$ was obtained from the pseudoscalar-baryon$(1/2^+)$ interaction, in accordance with results of Ref. [43]; also an extra sector of pseudoscalar-baryon$(3/2^+)$ could be related to the $\Omega_c(3119)$, therefore assigning to it the quantum numbers $J^P = 3/2^-$.

Other works on the molecular picture followed [50–52]. In Ref. [50] the authors propose that the broad structure found around 3188 MeV [1,2] could be related with a molecular ΞD state due to the proximity of its threshold around 3185 MeV. As we shall see in the next section, in our approach [44] the molecular state dominated by the ΞD channel corresponds to the $\Omega_c(3090)$.

In the present work we propose the experimental study of these new states through the decay of Ω_b^- baryons, as suggested in Ref. [53]. The mass and lifetime of the Ω_b^- were recently measured by the LHCb Collaboration [54], obtaining results compatible with the previous measurements of the same collaboration [55] and also with the ones of the CDF Collaboration [56], but not with the results of the D0 Collaboration [57]. We shall adopt the mass value listed by the Particle Data Group [58], which is quite close to the most recent measurement of LHCb.

We will discuss the decay $\Omega_b^- \to (\Xi_c^+ K^-)\pi^-$, which could be performed by the LHCb Collaboration [53] in the future and could be very useful to distinguish states with different structures and quantum numbers. First we present a brief summary of the main results of Ref. [44] and comment on the formalism employed there to obtain the $\Omega_c(3050)$ and $\Omega_c(3090)$ as meson-baryon molecules. Next we will discuss the $\Omega_b^- \to (\Xi_c^+ K^-)\pi^-$ decay and how the coupled channels approach naturally accounts for the dynamical generation of the Ω_c states from the hadronization that takes place after the conversion of the b quark into a c quark. Then we show the results of how these two states would be seen in the Ω_b^- decay if the molecular picture of Ref. [44] is correct, providing solid predictions that could easily be put to proof in the near future.

II. THE $\Omega_c(3050)$ AND $\Omega_c(3090)$ IN THE MOLECULAR PICTURE

In Ref. [44] a thorough discussion was made about the meson-baryon interaction due to the exchange of vector mesons, and an extension of the local hidden gauge approach [45–49] was used together with a method that takes into account the information of the spin-flavor wave functions of the baryons (see Ref. [44] for details). It was shown that considering the heavy quarks as spectators, the interactions can be obtained from the chiral Lagrangians using only $SU(3)$ symmetry [without the need of $SU(4)$ in the dominant terms], respecting heavy quark spin symmetry in the leading terms in the $(1/m_Q)$ counting where only light vectors are exchanged [59–61].

The procedure begins with the choice of meson-baryon channels in the $C = 1$, $S = -2$, and $I = 0$ sector, interacting in the S wave, with a determined total spin J. While vector-baryon contributions were also considered in Ref. [44], it was also shown there that these states decouple to a good degree of approximation from pseudoscalar-baryon states, and using the channels $\Xi_c\bar{K}$, $\Xi_c'\bar{K}$, ΞD, and $\Omega_c\eta$ the states $\Omega_c(3050)$ and $\Omega_c(3090)$ could be reproduced, both the mass and width.

In Ref. [44] the Bethe-Salpeter equation with the above channels was solved and poles were searched in the second Riemann sheet of the complex energy plane, with the results shown in Table I, where the couplings of the resonances to the different channels, g_i, are given, as well as the wave function at the origin $g_i G_i^{II}$, where G_i^{II} means the meson-baryon loop function evaluated at the pole position in the second Riemann sheet [44,62,63].

III. THE $\Omega_b^- \to (\Xi_c\bar{K}/\Xi_c'\bar{K}/\Xi D)\pi^-$ DECAYS

Let us see how the $\Omega_c(3050)$ and $\Omega_c(3090)$ are produced in this reaction within our picture. Since the resonances come from the interaction of pseudoscalar-baryon states shown in Table I, one has to hadronize the three quarks that come from the $b \to c$ transition and the spectator ss quarks (see Fig. 1). In the hadronization we introduce $\bar{q}q$ with the quantum numbers of the vacuum, and two options are possible: insertion of $\bar{q}q$ between the c and one s quark, as shown in the figure, or insertion between the two s quarks. In this latter case the three final quarks (leaving the π^- apart) have $J^P = 1/2^+$ and hence the state has positive parity. With one pseudoscalar, $J^P = 0^-$, and a baryon of $J^P = 1/2^+$ in the final state, this requires a P wave, but the molecules are produced in an S wave, and this mechanism is hence inoperative to produce these resonances. In the case of hadronization between the c and s quarks, the c quark can be produced in $L = 1$ after the weak vertex and the negative parity is restored. Then, the $L = 1$ excited c quark is deexcited via hadronization, where the $\bar{q}q$ is produced in a $^3P_0$ state [64–66].

Looking at the flavor of the quarks, the hadronization proceeds as follows:

$$css \to c(\bar{u}u + \bar{d}d + \bar{s}s)ss \equiv H, \tag{1}$$

$$H = \sum_i c\bar{q}_i q_i ss \equiv \sum_i \Phi_{4i} q_i ss, \tag{2}$$

where in the last step we have written the $(q\bar{q})$ matrix

TABLE I. Pole position [MeV], couplings g_i [dimensionless], and wave functions at the origin $g_i G_i^{II}$ [MeV] from pseudoscalar(0^-)-baryon($1/2^+$) interaction describing the $\Omega_c(3050)$ and $\Omega_c(3090)$.

3054.05 + i0.44	$\Xi_c \bar{K}$	$\Xi_c' \bar{K}$	ΞD	$\Omega_c \eta$
g_i	$-0.06 + i0.14$	**1.94 + i0.01**	$-2.14 + i0.26$	$1.98 + i0.01$
$g_i G_i^{II}$	$-1.40 - i3.85$	**−34.41 − i0.30**	$9.33 - i1.10$	$-16.81 - i0.11$
3091.28 + i5.12	$\Xi_c \bar{K}$	$\Xi_c' \bar{K}$	ΞD	$\Omega_c \eta$
g_i	$0.18 - i0.37$	$0.31 + i0.25$	**5.83 − i0.20**	$0.38 + i0.23$
$g_i G_i^{II}$	$5.05 + i10.19$	$-9.97 - i3.67$	**−29.82 + i0.31**	$-3.59 - i2.23$

$$(q\bar{q}) = \begin{pmatrix} u\bar{u} & u\bar{d} & u\bar{s} & u\bar{c} \\ d\bar{u} & d\bar{d} & d\bar{s} & d\bar{c} \\ s\bar{u} & s\bar{d} & s\bar{s} & s\bar{c} \\ c\bar{u} & c\bar{d} & c\bar{s} & c\bar{c} \end{pmatrix} \tag{3}$$

in terms of their meson components by means of the matrix Φ,

$$\Phi = \begin{pmatrix} \frac{\pi^0}{\sqrt{2}} + \frac{\eta}{\sqrt{3}} + \frac{\eta'}{\sqrt{6}} & \pi^+ & K^+ & \bar{D}^0 \\ \pi^- & -\frac{\pi^0}{\sqrt{2}} + \frac{\eta}{\sqrt{3}} + \frac{\eta'}{\sqrt{6}} & K^0 & D^- \\ K^- & \bar{K}^0 & -\frac{\eta}{\sqrt{3}} + \sqrt{\frac{2}{3}}\eta' & D_s^- \\ D^0 & D^+ & D_s^+ & \eta_c \end{pmatrix}. \tag{4}$$

In the matrix Φ we have included the mixing between η and η' [67].

Then replacing the $c\bar{q}$ meson terms we get

$$H = D^0 uss + D^+ dss + \cdots, \tag{5}$$

where we have already neglected the heavy combination of $D_s^+ sss$, which could only contribute to states with $J^P = 3/2^-$ since sss corresponds to the Ω^-, and furthermore its mass is far away from the range of energies studied here.

It is easy to see that, since ss has isospin zero, the combination $D^0 uss + D^+ dss$ has isospin zero,[1] and uss and dss have only overlap with Ξ^0 and Ξ^-, respectively. Hence the combination of Eq. (5) can be written up to a global factor by

$$H = |\Xi D, I = 0\rangle = -\frac{1}{\sqrt{2}}|\Xi^0 D^0 - \Xi^- D^+\rangle, \tag{6}$$

where we have absorbed the global minus sign when we changed to the isospin zero combination in the order baryon meson.

[1]Recall the isospin doublets:

$$D = \begin{pmatrix} D^+ \\ -D^0 \end{pmatrix}, \qquad \Xi = \begin{pmatrix} \Xi^0 \\ -\Xi^- \end{pmatrix}.$$

Now we proceed to construct the amplitude of the process $\Omega_b^- \to (\Xi_c \bar{K})\pi^-$. It is instructive to first look at the process $\Omega_b^- \to (\Xi D)\pi^-$, as depicted in Fig. 2. From Eq. (6) we see that after the emission of a pion, the hadronization involving the css quarks generates a ΞD pair in isospin zero. Thus we can write this process as the sum of a tree-level contribution and the final state interaction of ΞD going through the molecular states of Table I. This information is contained in the diagonal t matrix element $t^{I=0}_{\Xi D \to \Xi D}$, calculated in Ref. [44].

Then for the tree-level contribution (left diagram of Fig. 2) we simply write $t_{\rm tree} = V_P$, where V_P contains all information related to the Ω_b^- weak decay and dynamics of the hadronization, a common unknown factor in all processes we will investigate. On the other hand, for the ΞD rescattering (right diagram of Fig. 2) we will have

$$t_{\rm loop} = V_P G_{\Xi D}[M_{\rm inv}(\Xi D)] t^{I=0}_{\Xi D \to \Xi D}[M_{\rm inv}(\Xi D)], \tag{7}$$

where $G_{\Xi D}$ is the propagator of the baryon-meson loop, calculated in Ref. [44] as part of the Bethe-Salpeter equation, $T = [1 - VG]^{-1} V$ [68,69], with V the transition potential [44]. Then the amplitude of the process $\Omega_b^- \to \pi^- \Xi D$ is given by

$$t_{\Omega_b^- \to \pi^- \Xi D} = V_P [1 + G_{\Xi D}(M_{\Xi D}) t^{I=0}_{\Xi D \to \Xi D}(M_{\Xi D})], \tag{8}$$

where we introduced the compact notation $M_{\Xi D}$ for $M_{\rm inv}(\Xi D)$. With this amplitude we can write the ΞD invariant mass distribution

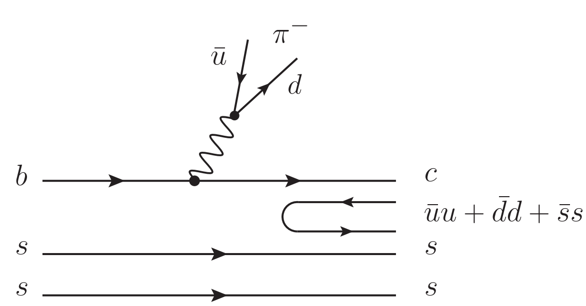

FIG. 1. Ω_b^- decay at quark level with emission of a π^- and subsequent hadronization.

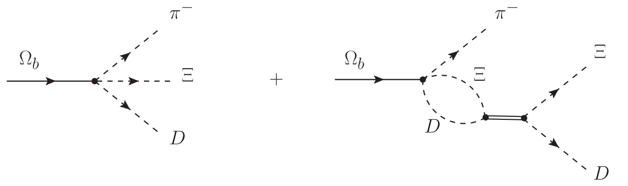

FIG. 2. $\Omega_b^- \to \pi^- \Xi D$ process. Tree level (left) plus ΞD rescattering (right).

$$\frac{d\Gamma}{dM_{\rm inv}(\Xi D)} = \frac{1}{(2\pi)^3} \frac{M_\Xi}{M_{\Omega_b^-}} p_{\pi^-} \tilde{p}_D |t_{\Omega_b^- \to \pi^- \Xi D}|^2, \qquad (9)$$

where we adopt the Mandl-Shaw normalization for fermions fields and p_{π^-} is the pion momentum in the Ω_b^- rest frame for the $\Omega_b^- \to (\Xi D)\pi^-$ decay

$$p_{\pi^-} = \frac{\lambda^{1/2}(M^2_{\Omega_b^-}, m_\pi^2, M^2_{\rm inv}(\Xi D))}{2M_{\Omega_b^-}}, \qquad (10)$$

and $\tilde{p}_D$ is the D momentum in the ΞD rest frame

$$\tilde{p}_D = \frac{\lambda^{1/2}(M^2_{\rm inv}(\Xi D), m_D^2, m_\Xi^2)}{2M_{\rm inv}(\Xi D)}. \qquad (11)$$

For the $\Omega_b^- \to (\Xi_c \bar{K})\pi^-$ process there is no tree-level contribution, since the hadronization only produces a ΞD pair, as in Eq. (6). Then the only contribution comes from the diagram in Fig. 3.

Because of our coupled channels approach, the transition $\Xi D \to \Xi_c \bar{K}$ is already contained in the t matrix and the production of $\Xi_c \bar{K}$ (also in isospin zero) appears naturally. The corresponding amplitude will be

$$t_{\Omega_b^- \to \pi^- \Xi_c \bar{K}} = V_P G_{\Xi D}(M_{\Xi_c \bar{K}}) t_{\Xi D \to \Xi_c \bar{K}}(M_{\Xi_c \bar{K}}), \qquad (12)$$

where $t_{\Xi D \to \Xi_c \bar{K}}$ is the transition amplitude of $\Xi D \to \Xi_c \bar{K}$, from the same t matrix. Then the $\Xi_c \bar{K}$ invariant mass distribution is also analogous,

$$\frac{d\Gamma}{dM_{\rm inv}(\Xi_c \bar{K})} = \frac{1}{(2\pi)^3} \frac{M_{\Xi_c}}{M_{\Omega_b^-}} p_{\pi^-} \tilde{p}_{\bar{K}} |t_{\Omega_b^- \to \pi^- \Xi_c \bar{K}}|^2, \qquad (13)$$

where p_{π^-} is the pion momentum in the Ω_b^- rest frame [now for $\Omega_b^- \to (\Xi_c \bar{K})\pi^-$] and $\tilde{p}_{\bar{K}}$ is the kaon momentum in the $\Xi_c \bar{K}$ rest frame, analogous to Eqs. (10) and (11).

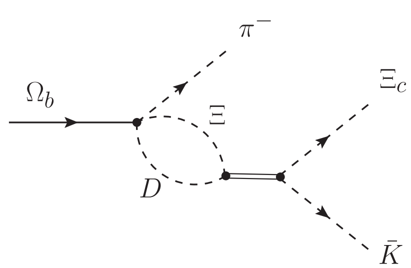

FIG. 3. $\Omega_b^- \to \pi^- \Xi_c \bar{K}$ process through ΞD rescattering.

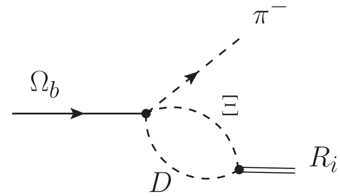

FIG. 4. Resonance coalescence in the $\Omega_b^- \to \pi^- R_i$ process through ΞD rescattering, where R_i is the $\Omega_c(3050)$ or $\Omega_c(3090)$.

Analogously, we can also calculate the invariant mass distribution for the final state $\Xi_c' \bar{K}$, replacing Ξ_c by Ξ_c' in the previous equations and taking the matrix element of the t matrix corresponding to the transition $\Xi D \to \Xi_c' \bar{K}$.

It is also interesting to look at the case of coalescence, where the ΞD pair merges into the resonance regardless of the final decay channel, as depicted in Fig. 4.

The value of the amplitude in the process $\Omega_b^- \to \pi^- R_i$, where R_i is one of the molecular states of Table I, is proportional to the coupling of that resonance to the ΞD channel,

$$t_{\Omega_b^- \to \pi^- R_i} = V_P G_{\Xi D}(M_{R_i}) g_{R_i, \Xi D}, \qquad (14)$$

where the propagator is calculated at the resonance mass M_{R_i}. With this quantity we can calculate the equivalent of the integrated mass distribution around the R_i resonance, which does not depend on its decay mode,

$$\Gamma_{\Omega_b^- \to \pi^- R_i} = \frac{1}{2\pi} \frac{M_{R_i}}{M_{\Omega_b^-}} p'_{\pi^-} |t_{\Omega_b^- \to \pi^- \Xi_c \bar{K}}(M_{R_i})|^2, \qquad (15)$$

where p'_{π^-} is the pion momentum in the Ω_b^- rest frame for $\Omega_b^- \to \pi^- R_i$.

Let us make some further remarks concerning the Ω_b decay process. As we have discussed, the mechanism of Fig. 2 or 3 produces the resonances $\Omega_c(3050)$ and $\Omega_c(3090)$. These resonances are generated in Ref. [44] through the interaction of the coupled channels $\Xi_c \bar{K}$, $\Xi_c' \bar{K}$, ΞD, and $\Omega_c \eta$. The approach of Ref. [44] takes into account the transition from one channel to another, and all of them participate in the generation of the resonances. In principle one could create these resonances initiated by any of the channels. However, the discussion leading to Eq. (6) tells us that the weak decay mechanism filters the primary production of the ΞD channel and the resonances are only initiated by this channel. This does not mean that the other channels do not play a role here. Their contribution is implicit in the $t_{\Xi D \to {\rm final}}$ transition amplitudes, which contain all channels through the terms $V_{\Xi D \to i} G_i V_{i \to {\rm final}}$, $V_{\Xi D \to i} G_i V_{ij} G_j V_{j \to {\rm final}}$, etc., that are summed up by the Bethe-Salpeter equation.

One can, however, see if there is a way to produce, for instance, $\Xi_c \bar{K}$ in the first step of the decay. Topologically this is possible producing the hadronization between the ss quarks in Fig. 1. Indeed, taking the $\bar{u}u$ component of the hadronization one obtains the cus baryon, corresponding to Ξ_c and $\bar{u}s$ that corresponds to K^-. However, in the spectator picture of Fig. 1 this is not possible for other reasons, as we pointed out above. Indeed, since the c quark is not affected by the hadronization and belongs to Ξ_c at the end, it is a state $1/2^+$ in its ground state. But the initial ss component is a spectator in the weak decay and both quarks are in $1/2^+$ and ground state. After the weak decay and prior to the hadronization we have c, s, s all in $1/2^+$ and in their ground state, and have total positive parity. This state cannot lead to the $1/2^-$ $\Omega_c(3050)$, $\Omega_c(3090)$ resonances, or equivalently meson baryon in the S wave.

IV. RESULTS

It is interesting to see how these processes show the importance of the coupled channels. The decay of the Ω_c states into ΞD is kinematically forbidden below the corresponding threshold at 3185 MeV; then we cannot see the corresponding peaks in the ΞD invariant mass distribution, but we can see their indirect effect, both from the meson-baryon loop in Eq. (8) and from the amplitude $t^{I=0}_{\Xi D\to\Xi D}$. The corresponding invariant mass distribution, Eq. (9), is shown in Fig. 5 by the solid line. To compare with the case where only the tree-level contributes, we remove $t_{\rm loop}$ and keep only $t_{\rm tree}$ [keeping only the term 1 in the bracket of Eq. (8)], normalizing the curve such that it has the same area as the solid curve in the energy range shown, which is plotted as the dashed line in Fig. 5. We should note that, should we have produced the ΞD in the P wave at tree level, hadronizing with $\bar{q}q$ within the two s quarks, we would find a contribution to $d\Gamma/dM_{\rm inv}(\Xi D)$ in Eq. (9) with an extra $\tilde{p}_D^2$ factor, which changes the shape of the dashed line in Fig. 5 drastically and is easily distinguishable from an S wave.

If we look at $\pi^-\Xi_c\bar{K}$ in the final state, the $\Xi_c\bar{K}$ threshold is at 2965 MeV, and then we can see clearly the peaks of the Ω_c states in the $\Xi_c\bar{K}$ invariant mass distribution. According to Eq. (6), we expect only ΞD production from the hadronization that occurs right after the Ω_b^- decay, which means we have no tree-level contribution for $\Xi_c\bar{K}$ production. However, the transition to $\Xi_c\bar{K}$ through off-shell ΞD loops arises naturally from the coupled channels approach. In fact, both the $\Omega_c(3050)$ and the $\Omega_c(3090)$ couple strongly to ΞD (see Table I), and their formation from the ΞD state formed in the first step of the Ω_b^- decay with subsequent transition to $\Xi_c\bar{K}$ (going through the ΞD virtual state) is not only possible, but expected.

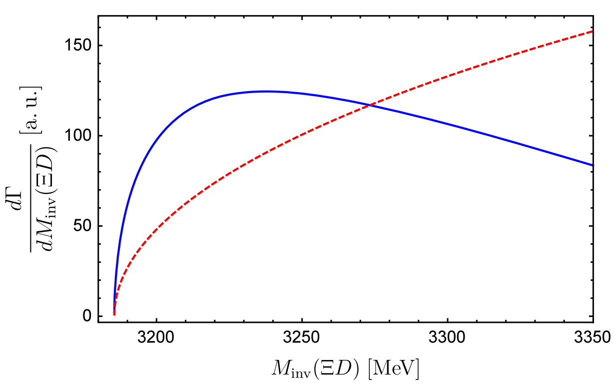

FIG. 5. ΞD invariant mass distribution from Eq. (9). Solid line: Using the complete amplitude of Eq. (8). Dashed line: Removing the $G_{\Xi D}t^{I=0}_{\Xi D\to\Xi D}$ term (only tree-level contribution) and normalizing such that both curves have the same area.

In Fig. 6 we show the $\Xi_c\bar{K}$ invariant mass distribution. The only unknown quantity is the global factor V_P, common to all amplitudes we investigate here. The ratio between the intensity of each peak does not depend on V_P, so all ratios are predictions that could be confronted with future experiments. We can see that the intensity of the $\Omega_c(3050)$ peak is about 65% higher than for the $\Omega_c(3090)$ peak.

The width of the states in Fig. 6 is an output of the coupled channels dynamics in Ref. [44] to generate the Ω_c states. However, as seen in Fig. 3, the strength of these peaks is related to the product of the couplings of the resonances to ΞD and $\Xi_c\bar{K}$ and hence is a direct consequence of the way in which the reaction proceeds according to our picture.

Note that we are using the same normalization for all the reactions; hence the ratio of the strength at the peaks in Fig. 6 to the strength of the ΞD mass distribution (solid line) in Fig. 5 is also a prediction. In arbitrary units, the ΞD distribution has a maximum of about 125 around 3240 MeV, whereas in the $\Xi_c\bar{K}$ distribution the $\Omega_c(3050)$ and $\Omega_c(3090)$ peaks have an intensity of about 15.50×10^3 and 9.45×10^3, respectively, therefore we predict that the $\Xi_c\bar{K}$ distribution in the vicinity of the resonance peaks is roughly 2 orders of magnitude higher than that of the ΞD distribution.

Cusp effects in the $\Xi_c\bar{K}$ distribution also appear at the $\Xi_c'\bar{K}$ and ΞD thresholds at 3074 MeV and 3185 MeV, respectively, but their intensity is very small compared to the peaks of the resonances and cannot be seen clearly in Fig. 6. Then, according to our predictions they should not be seen in experiment.

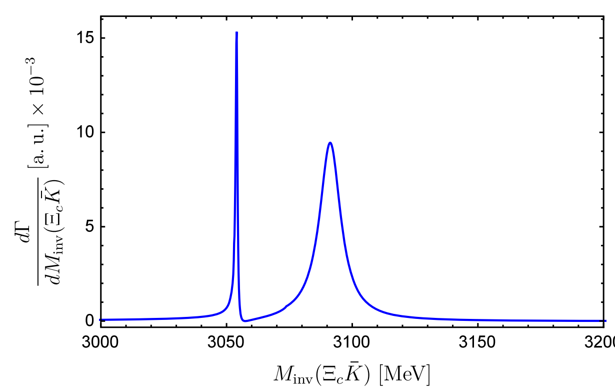

FIG. 6. $\Xi_c\bar{K}$ invariant mass distribution from Eq. (13).

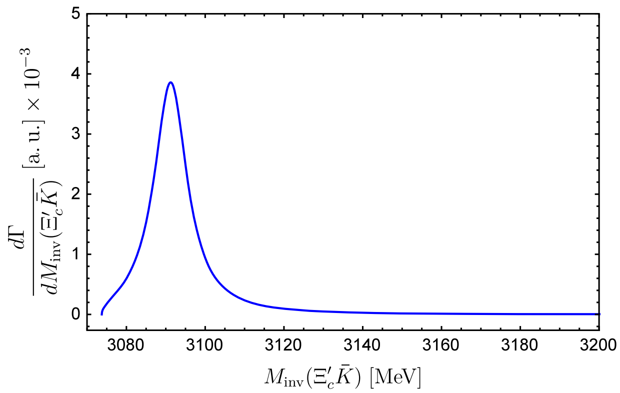

FIG. 7. $\Xi'_c\bar{K}$ invariant mass distribution from Eq. (13), replacing Ξ_c by Ξ'_c and taking $t_{\Xi D\to\Xi'_c\bar{K}}$.

We also notice that apparently no significant interference pattern is seen between the two states in Fig. 6, even though they have the same quantum numbers, a feature that also agrees with the fit performed by the LHCb Collaboration [1,16].

As for the $\Xi'_c\bar{K}$ invariant mass distribution, only the $\Omega_c(3090)$ can be seen, as shown in Fig. 7, since this channel is also open for the decay of this state, whereas the $\Omega_c(3050)$ is below the threshold of $\Xi'_c\bar{K}$.

Again we can compare the intensity of the peaks. In the $\Xi'_c\bar{K}$ distribution the $\Omega_c(3090)$ peak has an intensity of 3.86×10^3, which is about 40% of the intensity it has in the $\Xi_c\bar{K}$.

Finally, it is interesting to compare the results of $\Gamma_{\Omega_b^-\to\pi^-R_i}$, given by Eq. (15), with the integrated invariant mass distribution of Eq. (13) around the peak of each resonance,

$$\int_{R_i}\frac{d\Gamma}{dM_{\mathrm{inv}}(\Xi_c\bar{K})}dM_{\mathrm{inv}}(\Xi_c\bar{K}). \tag{16}$$

In Table II we show the results of Eqs. (15) and (16) for the $\Omega_c(3050)$ and $\Omega_c(3090)$, and for the latter we also show the integrated $\Xi'_c\bar{K}$ distribution.

From these results we can draw some interesting conclusions. Let us look first at the $\Omega_c(3050)$. In Table I we can see that this state is dominated by the $\Xi'_c\bar{K}$ channel, and also has sizable contributions from the higher channels ΞD and $\Omega_c\eta$. However, the pole is at 3054 MeV, which is 20 MeV below the $\Xi'_c\bar{K}$ threshold, so the only open channel is $\Xi_c\bar{K}$, to which the resonance couples very weakly and the phase space available is only about 90 MeV. This feature explains two points: (1) The narrowness of the state, whose upper limit of the width reported by the LHCb Collaboration is $0.8\pm 0.2\pm 0.1$ MeV [1], in excellent agreement with the result of Ref. [44] with $\Gamma = 2\times\mathrm{Im}(R_i) = 0.88$ MeV; (2) The good agreement of $\Gamma_{\Omega_b^-\to\pi^-R_i}$, 21289, given by Eq. (15), with the integrated invariant mass distribution around the resonance peak, 21344, given by Eq. (16) (the small difference is irrelevant and comes essentially from the choice of the interval of integration). This happens because the state is very narrow and the only channel open for decay is the $\Xi_c\bar{K}$, so the value we obtain from the coalescence, which is independent of the decay channel, matches the value obtained from the integration over the only channel available ($\Xi_c\bar{K}$), as it should be.

TABLE II. Comparison between integrated invariant mass distributions around each resonance and the corresponding coalescence (arbitrary units).

State	$\Omega_c(3050)$	$\Omega_c(3090)$	
Pole [MeV]	**3054.05 + i0.44**	**3091.28 + i5.12**	
Coalescence Eq. (15)	21289	215237	
Channel	$\Xi_c\bar{K}$	$\Xi_c\bar{K}$	$\Xi'_c\bar{K}$
Interval [MeV]	[3049, 3057]	[3057, 3120]	[3074, 3120]
Integral Eq. (16)	21344	133482	51074

On the other hand, the $\Omega_c(3090)$ is dominated by the ΞD channel, with some contribution from the other channels. Even though this state couples very strongly to ΞD, it is almost 100 MeV below the respective threshold. It can only decay to $\Xi_c\bar{K}$ and $\Xi'_c\bar{K}$. In both cases the coupling is small, and in the latter channel the phase space available is less than 20 MeV (see Table I). This again, explains two main features: (1) The narrowness, with a width not so small as in the case of the $\Omega_c(3050)$, but still very narrow, since the decay into $\Xi_c\bar{K}$ is reasonable, with more than 120 MeV of phase space available, although the coupling to that channel is weak. The LHCb reports a width of $8.7\pm 1.0\pm 0.8$ MeV [1], in fair agreement with the result of Ref. [44] of 10.24 MeV; (2) The fact that the integrated invariant mass distribution around the peak, 133482 in the $\Xi_c\bar{K}$ distribution, is about 2/3 of the total given by the coalescence, 215237, which is also expected, since in Eq. (16) we are integrating only in the $\Xi_c\bar{K}$ channel, whereas this state can also decay into $\Xi'_c\bar{K}$. The sum of both integrals, in $\Xi_c\bar{K}$ and $\Xi'_c\bar{K}$, is 184556, close to the total given by the coalescence, but still below. This is also expected since Eq. (15) is actually an approximation that is valid in the limit of zero width, which works pretty well for the $\Omega_c(3050)$ but is not so good for the $\Omega_c(3090)$, with already 10 MeV of width.

As a prediction we can also state, based on the coalescence results, that the ratio of the $\Omega_c(3050)$ over the $\Omega_c(3090)$ production is about 10% in the Ω_b^- decay:

$$\frac{\Gamma_{\Omega_b^-\to\pi^-\Omega_c(3050)}}{\Gamma_{\Omega_b^-\to\pi^-\Omega_c(3090)}}\approx 10\%. \tag{17}$$

Another point worth discussing is the possibility to have some component of these resonances of the $3q$ type and not molecular. We have considered Ω_c states of pure molecular nature. In the real world, if allowed by quantum numbers, the mixing with $3q$ components with the same quantum numbers is unavoidable. The question is how large these components are. In our work we are implicitly assuming that they are negligible. The issue of the mixing of $3q$ and molecular components has received some attention [70–72], and present lattice results [73] are helping in these studies through proper analysis, as done in Ref. [72]. These studies show that in cases where the dynamical coupled channels unitary approach leads to molecular states, the $3q$ components are indeed small. Yet, the question here is whether we can show how the present results are stable under the assumption of small $3q$ components for the Ω_c states. An answer for this problem is already available in the thorough study carried out in Ref. [74].

In that work a study similar to the present one is carried out for the $B_s^0 \to J/\Psi f_1(1285)$ decay. The J/Ψ plays the role of the pion here, and the $f_1(1285)$ state, assumed to be a $K^*\bar{K}$ molecule, plays the role of the Ω_c resonances here. In Ref. [74] a study was done taking into account the $f_1(1285)$ as a pure molecule or heaving a probability z to be a $q\bar{q}$ state. The details of the issue are shown in Sec. IX of Ref. [74] where one can see that for values of $z \approx 0.2$ the changes in ratios of magnitudes are smaller than 20% and they are also moderate for values of $z \approx 0.4$. These results tell us that the results obtained here are solid in this respect, since changes of 20% in the results obtained are not relevant for the prospective work carried out here.

V. CONCLUSIONS

We have studied the weak decay $\Omega_b^- \to (\Xi_c^+ K^-)\pi^-$, in view of the narrow Ω_c states recently measured by the LHCb Collaboration and later confirmed by the Belle Collaboration. Based on the previous work where the $\Omega_c(3050)$ and $\Omega_c(3090)$ are described as meson-baryon molecular states, using an extension of the local hidden gauge approach in coupled channels, with results in remarkable agreement with experiment, we have investigated the ΞD, $\Xi_c \bar{K}$, and $\Xi_c' \bar{K}$ invariant mass distributions and discussed the role of coupled channels in the process. Predictions that could be confronted with future experiments are presented, providing useful information that could help to determine the quantum numbers and nature of these states. Since Ω_b^- baryons have already been observed in several experiments, two of them performed by the LHCb Collaboration, the present work should encourage such study in the near future, which would certainly bring novel key information for the understanding of these new states.

ACKNOWLEDGMENTS

V. R. D. acknowledges the Programa Santiago Grisolia of Generalitat Valenciana (Exp. GRISOLIA/2015/005) and the discussions with I. Belyaev and S. Neubert. J. M. D. thanks the Fundação de Amparo à Pesquisa do Estado de São Paulo (FAPESP) for support by FAPESP Grant No. 2016/22561-2. This work is partly supported by the National Natural Science Foundation of China (NSFC) under Grants No. 11565007 and No. 11747307. This work is also partly supported by the Spanish Ministerio de Economia y Competitividad and European Fundacion Europea para el desarrollo regional (FEDER) funds under Contracts No. FIS2014-57026-REDT, No. FIS2014-51948-C2-1-P, and No. FIS2014-51948-C2-2-P, and the Generalitat Valenciana in the program Prometeo II-2014/068.

[1] R. Aaij *et al.* (LHCb Collaboration), Phys. Rev. Lett. **118**, 182001 (2017).
[2] J. Yelton *et al.* (Belle Collaboration), Phys. Rev. D **97**, 051102 (2018).
[3] D. Ebert, R. N. Faustov, and V. O. Galkin, Phys. Lett. B **659**, 612 (2008).
[4] W. Roberts and M. Pervin, Int. J. Mod. Phys. A **23**, 2817 (2008).
[5] H. Garcilazo, J. Vijande, and A. Valcarce, J. Phys. G **34**, 961 (2007).
[6] S. Migura, D. Merten, B. Metsch, and H. R. Petry, Eur. Phys. J. A **28**, 41 (2006).
[7] D. Ebert, R. N. Faustov, and V. O. Galkin, Phys. Rev. D **84**, 014025 (2011).
[8] A. Valcarce, H. Garcilazo, and J. Vijande, Eur. Phys. J. A **37**, 217 (2008).
[9] Z. Shah, K. Thakkar, A. K. Rai, and P. C. Vinodkumar, Chin. Phys. C **40**, 123102 (2016).
[10] J. Vijande, A. Valcarce, T. F. Carames, and H. Garcilazo, Int. J. Mod. Phys. E **22**, 1330011 (2013).
[11] T. Yoshida, E. Hiyama, A. Hosaka, M. Oka, and K. Sadato, Phys. Rev. D **92**, 114029 (2015).
[12] H. X. Chen, W. Chen, Q. Mao, A. Hosaka, X. Liu, and S. L. Zhu, Phys. Rev. D **91**, 054034 (2015).
[13] H. X. Chen, Q. Mao, A. Hosaka, X. Liu, and S. L. Zhu, Phys. Rev. D **94**, 114016 (2016).
[14] G. Chiladze and A. F. Falk, Phys. Rev. D **56**, R6738 (1997).
[15] A. Manohar and H. Georgi, Nucl. Phys. **B234**, 189 (1984).
[16] M. Karliner and J. L. Rosner, Phys. Rev. D **95**, 114012 (2017).
[17] B. Chen and X. Liu, Phys. Rev. D **96**, 094015 (2017).
[18] W. Wang and R. L. Zhu, Phys. Rev. D **96**, 014024 (2017).
[19] K. L. Wang, L. Y. Xiao, X. H. Zhong, and Q. Zhao, Phys. Rev. D **95**, 116010 (2017).

[20] A. Ali, L. Maiani, A. V. Borisov, I. Ahmed, M. J. Aslam, A. Y. Parkhomenko, A. D. Polosa, and A. Rehman, Eur. Phys. J. C **78**, 29 (2018).
[21] S. S. Agaev, K. Azizi, and H. Sundu, Europhys. Lett. **118**, 61001 (2017).
[22] H. X. Chen, Q. Mao, W. Chen, A. Hosaka, X. Liu, and S. L. Zhu, Phys. Rev. D **95**, 094008 (2017).
[23] Z. G. Wang, Eur. Phys. J. C **77**, 325 (2017).
[24] T. M. Aliev, S. Bilmis, and M. Savci, arXiv:1704.03439.
[25] S. S. Agaev, K. Azizi, and H. Sundu, Eur. Phys. J. C **77**, 395 (2017).
[26] Q. Mao, H. X. Chen, A. Hosaka, X. Liu, and S. L. Zhu, Phys. Rev. D **96**, 074021 (2017).
[27] Z. G. Wang, X. N. Wei, and Z. H. Yan, Eur. Phys. J. C **77**, 832 (2017).
[28] M. Padmanath and N. Mathur, Phys. Rev. Lett. **119**, 042001 (2017).
[29] G. Yang and J. Ping, Phys. Rev. D **97**, 034023 (2018).
[30] H. Huang, J. Ping, and F. Wang, Phys. Rev. D **97**, 034027 (2018).
[31] H. C. Kim, M. V. Polyakov, and M. Praszałowicz, Phys. Rev. D **96**, 014009 (2017); **96**, 039902(E) (2017).
[32] C. S. An and H. Chen, Phys. Rev. D **96**, 034012 (2017).
[33] A. Ali, J. S. Lange, and S. Stone, Prog. Part. Nucl. Phys. **97**, 123 (2017).
[34] V. V. Anisovich, M. A. Matveev, J. Nyiri, and A. N. Semenova, Mod. Phys. Lett. A **32**, 1750154 (2017).
[35] Z. Zhao, D. D. Ye, and A. Zhang, Phys. Rev. D **95**, 114024 (2017).
[36] K. L. Wang, Y. X. Yao, X. H. Zhong, and Q. Zhao, Phys. Rev. D **96**, 116016 (2017).
[37] H. C. Kim, M. V. Polyakov, M. Praszałowicz, and G. S. Yang, Phys. Rev. D **96**, 094021 (2017).
[38] H. Y. Cheng and C. W. Chiang, Phys. Rev. D **95**, 094018 (2017).
[39] J. Hofmann and M. F. M. Lutz, Nucl. Phys. **A763**, 90 (2005).
[40] C. E. Jimenez-Tejero, A. Ramos, and I. Vidana, Phys. Rev. C **80**, 055206 (2009).
[41] O. Romanets, L. Tolos, C. Garcia-Recio, J. Nieves, L. L. Salcedo, and R. G. E. Timmermans, Phys. Rev. D **85**, 114032 (2012).
[42] J. Nieves, R. Pavao, and L. Tolos, Eur. Phys. J. C **78**, 114 (2018).
[43] G. Montana, A. Feijoo, and A. Ramos, Eur. Phys. J. A **54**, 64 (2018).
[44] V. R. Debastiani, J. M. Dias, W. H. Liang, and E. Oset, Phys. Rev. D **97**, 094035 (2018).
[45] M. Bando, T. Kugo, S. Uehara, K. Yamawaki, and T. Yanagida, Phys. Rev. Lett. **54**, 1215 (1985).
[46] M. Bando, T. Kugo, and K. Yamawaki, Phys. Rep. **164**, 217 (1988).
[47] U. G. Meißner, Phys. Rep. **161**, 213 (1988).
[48] M. Harada and K. Yamawaki, Phys. Rep. **381**, 1 (2003).
[49] H. Nagahiro, L. Roca, A. Hosaka, and E. Oset, Phys. Rev. D **79**, 014015 (2009).
[50] C. Wang, L. L. Liu, X. W. Kang, X. H. Guo, and R. W. Wang, Eur. Phys. J. C **78**, 407 (2018).
[51] R. Chen, A. Hosaka, and X. Liu, Phys. Rev. D **97**, 036016 (2018).
[52] Y. Huang, C. j. Xiao, Q. F. Lü, R. Wang, J. He, and L. Geng, Phys. Rev. D **97**, 094013 (2018).
[53] I. Belyaev, Spectroscopy of charm baryons at LHCb (2017), https://indico.cern.ch/event/578804/contributions/2636994/.
[54] R. Aaij *et al.* (LHCb Collaboration), Phys. Rev. D **93**, 092007 (2016).
[55] R. Aaij *et al.* (LHCb Collaboration), Phys. Rev. Lett. **110**, 182001 (2013).
[56] T. A. Aaltonen *et al.* (CDF Collaboration), Phys. Rev. D **89**, 072014 (2014).
[57] V. M. Abazov *et al.* (D0 Collaboration), Phys. Rev. Lett. **101**, 232002 (2008).
[58] C. Patrignani *et al.* (Particle Data Group), Chin. Phys. C **40**, 100001 (2016).
[59] N. Isgur and M. B. Wise, Phys. Lett. B **232**, 113 (1989).
[60] M. Neubert, Phys. Rep. **245**, 259 (1994).
[61] A. V. Manohar and M. B. Wise, *Heavy Quark Physics* (Cambridge University Press, Cambridge, 2000); Camb. Monogr. Part. Phys. Nucl. Phys. Cosmol. **10**, 1 (2000).
[62] D. Gamermann, J. Nieves, E. Oset, and E. R. Arriola, Phys. Rev. D **81**, 014029 (2010).
[63] F. Aceti and E. Oset, Phys. Rev. D **86**, 014012 (2012).
[64] L. Micu, Nucl. Phys. **B10**, 521 (1969).
[65] A. Le Yaouanc, L. Oliver, O. Pene, and J. C. Raynal, Phys. Rev. D **8**, 2223 (1973).
[66] W. H. Liang, M. Bayar, and E. Oset, Eur. Phys. J. C **77**, 39 (2017).
[67] A. Bramon, A. Grau, and G. Pancheri, Phys. Lett. B **283**, 416 (1992).
[68] J. A. Oller and E. Oset, Phys. Rev. D **60**, 074023 (1999).
[69] J. A. Oller and U. G. Meißner, Phys. Lett. B **500**, 263 (2001).
[70] A. M. Torres, E. Oset, S. Prelovsek, and A. Ramos, J. High Energy Phys. 05 (2015) 153.
[71] P. G. Ortega, J. Segovia, D. R. Entem, and F. Fernandez, Phys. Rev. D **94**, 074037 (2016).
[72] M. Albaladejo, P. Fernandez-Soler, J. Nieves, and P. G. Ortega, Eur. Phys. J. C **78**, 722 (2018).
[73] G. S. Bali, S. Collins, A. Cox, and A. Schäfer, Phys. Rev. D **96**, 074501 (2017).
[74] R. Molina, M. Döring, and E. Oset, Phys. Rev. D **93**, 114004 (2016).